

PAPER • OPEN ACCESS

## A model and simulation of lattice vibrations in a superabundant vacancy phase of palladium–deuterium

To cite this article: M R Staker 2020 *Modelling Simul. Mater. Sci. Eng.* **28** 065006

View the [article online](#) for updates and enhancements.



**IOP | ebooks™**

Bringing together innovative digital publishing with leading authors from the global scientific community.

Start exploring the collection—download the first chapter of every title for free.

# A model and simulation of lattice vibrations in a superabundant vacancy phase of palladium–deuterium

M R Staker 

Department of Engineering, Loyola University Maryland, 4501 North Charles St, Baltimore, MD, 21210, United States of America  
American Patent Institute, 2817 Wesleyan Drive, Churchville, MD 21028, United States of America

E-mail: [m.r.staker@alum.mit.edu](mailto:m.r.staker@alum.mit.edu) and [mstaker@loyola.edu](mailto:mstaker@loyola.edu)

Received 15 March 2020, revised 22 May 2020

Accepted for publication 4 June 2020

Published 10 July 2020



CrossMark

## Abstract

A one dimensional Bravais lattice model is applied to a superabundant vacancy (SAV) delta  $\delta$  phase ( $\text{Pd}_3\text{VacD}_4$ —octahedral), in the palladium–deuterium system. SolidWorks is used to simulate the motion of atoms and ions in the lattice. These two approaches give identical results for the vibrations of the deuterons indicating that large vibrations of deuterons are possible when the microstructure is a mixture of beta deuteride and small volume percent delta SAV phase. These conditions result from the unique geometry and crystallography of  $\delta$  phase. According to both the model and simulation, as the size of  $\delta$  phase increases, opportunity for high amplitude vibrations of deuterons increases. Increasing temperature should have a similar effect.

Keywords: superabundant vacancy structures, palladium–isotopic hydrogen phases, delta  $\delta$  and delta prime  $\delta'$  phases, lattice vibrations, resonance frequency, phonons

(Some figures may appear in colour only in the online journal)

## 1. Introduction

Superabundant vacancy phases (SAV) offer unique crystallography because the high levels of vacancies ( $\sim 25\%$ ) are ordered [1–21]. In the ordered  $\text{Pd}_3\text{VacD}_4$  SAV phase, deuterium (D) occupies octahedral interstitial sites of the palladium (Pd) face centered cubic structure (fcc)



Original content from this work may be used under the terms of the [Creative Commons Attribution 4.0 licence](https://creativecommons.org/licenses/by/4.0/). Any further distribution of this work must maintain attribution to the author(s) and the title of the work, journal citation and DOI.

as positive deuterons ( $D^+$ ), and vacancies ( $Vac^-$ ) occupying all unit cell corners with some negative charge. This phase, called delta ( $\delta$ ) phase, is located on the Pd–D phase diagram [22, 23] at a nominal D/Pd ratio of 1.33. The unique feature is orthogonal empty channels, along contiguous unit cell edges,  $\langle 100 \rangle$  directions, occupied only by regularly spaced deuterons with spacing equal to the unit cell lattice parameter. If the deuterons migrate to tetrahedral interstitial sites [24–26], the SAV phase is  $\delta'$  [22, 23], with empty channels or vacancy tubes with apparent enhanced electronic conduction [23]. In either case, diameters of these tubes vary periodically when traversing  $\langle 100 \rangle$  directions along contiguous unit cells. Its diameter ranges from a minimum of 0.414 of the Pd atom at the edge midpoint of the fcc unit cell (octahedral position), to a maximum value of the diameter of the Pd atom at corners of the unit cell [23]. Ignoring hydrogen, invisible to x-rays, and with ordered  $Vac^-$ , the unit cell of SAV phases is simple cubic (sc).

The properties of the SAV phases are not well known except: (1) the crystallography from x-ray diffraction, (2) unit cell dimensional behavior (contraction upon formation from the beta ( $\beta$ ) deuteride or hydride phase), and (3) thermal desorption spectral behavior [1–23]. Three reasons for lack of characterization are: difficulty achieving proper activity levels for SAV phases with electrolysis, the kinetics for their formation in the bulk is slow resulting in very small volume fractions, and their discovery was fairly recent.

The deuterons within the tubes of  $\delta$  phase can be regarded (and modeled) as a case of a one dimensional Bravais lattice of ions which has been described in solid state physics texts [27–29]. This paper develops such a model, examines longitudinal lattice vibrations of deuterons along edges of the unit cell, and uses a commercially available solid modeling computer-aided design software package (SolidWorks published by Dassault Systèmes with settings listed in appendix A) to simulate these vibrations (frequencies, amplitudes and velocities) within the tubes.

## 2. Analysis and model development

A one dimensional row of ions in a monatomic Bravais lattice, after Dean [30] and Ashcraft and Mermin [27], is shown in figure 1(a). Each ion of mass  $m$  is tied to its neighbor with ideal Hookean massless springs with only nearest neighbor forces considered. All springs and ions are connected, so the extreme end springs are viewed as being connected back to the beginning of the string by a loop with a large number of ions with the end spring (on the right) connected to the beginning ion (on left). Alternatively, connectivity is realized by a massless, perfectly rigid bar (figure 1(a)), capable of motion, assuring any motion on either extreme end is replicated at the opposite extreme end, as in the loop version.

With these end conditions, which assure connectivity from ion to ion only, Newton's second law of motion is applied longitudinally to each ion in the string and yields a dispersion relation of lattice waves or phonons [27, 28, 30] relating circular frequency  $\omega$  ( $\text{rad s}^{-1}$ ) for normal modes of vibration to the wave vector  $q$  and the ion lattice constant  $a$  as:

$$\omega = 2 \omega_0 \sin(qa/2). \quad (1)$$

Here  $\omega_0$  is  $(k/m)^{1/2}$ , the square root of the ratio of the Hookean spring constant  $k$  to the mass  $m$  of the ion and is considered the fundamental circular frequency ( $\text{rad s}^{-1}$ ). This dispersion relation assumes a large number of ions and is suitable for monolithic microstructures, but is untenable in this model where phase boundaries pose different string end conditions, and SAV size is often limited from kinetics and processing conditions. To account for phase boundaries and finite number of ions, end conditions are altered: the extreme right and extreme left springs

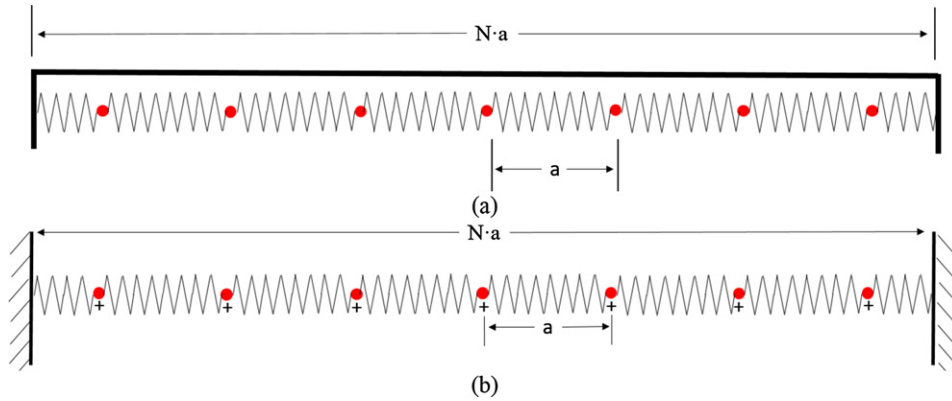


**Figure 1.** (a) A model of ions of mass  $m$  in a one-dimensional Bravais lattice where each ion is tied to its neighbor with an ideal Hookean massless spring with force constant  $k$  and only nearest neighbor forces are considered. Here the extreme ends of the springs are connected to a massless and infinitely ridged bar capable of motion, where the motion of one extreme end of the lattice is reproduced at the opposite extreme end of the lattice. Ions have a spacing (lattice constant) of  $a$ , and the total length of the string of  $N$  ions is  $N \cdot a$ . (b) Here the extreme ends of the springs are fixed, a built-in condition, lending the solution suitable for small finite number  $N$  of ions.

are fixed to rigid constraints (built-in and motionless) as shown in figure 1(b). Then the exact dispersion relation from Kittel [28] and Torre [29] becomes:

$$\omega = 2 \omega_0 \sin(m\pi/2(N + 1)) \quad (2)$$

where  $N$  is the total finite integral number of ions in the string. Each ion is numbered as  $m$ , so  $m$  is integral,  $1 \leq m \leq N$ , and called the mode number of the vibration. This relation is exact for all  $m$  and  $N$ , even if  $N$  is small, e.g. 3 to 10, and has the conditions of figure 1(b) with end conditions fixed and excited with a forcing function on one end (see discussion section for condition of forced vibration at both ends). This is useful since the total number of ions,  $N^3$ , in isolated particles of  $\delta$  phase, and their volume  $(N \cdot a)^3$ , have been shown to be a very small (e.g. 0.03%) volume fraction of the bulk [22, 23]. These small particles of  $\delta$  phase, distributed within the bulk, are consistent with nucleation and growth mechanisms.

Equation (2) is evaluated for each mode  $m$  and any  $N$  to yield a ratio of normal mode  $\omega$  to fundamental circular frequency,  $\omega/\omega_0$ . Thus the string has other normal modes, also called natural circular frequencies  $\omega$  [or frequencies  $f = (1/2\pi) \cdot \omega$ , in Hz], in addition to the fundamental circular frequency  $\omega_0$  [or fundamental frequency  $f_0 = (1/2\pi) \cdot \omega_0$ ]. Figure 2 shows equation (2) solutions of natural frequencies  $f$  for selected  $m$  modes and  $N$  ions. For any  $N$ , there are  $N$  natural frequencies, one for each  $m$ , consistent with string length  $(N \cdot a)$ . If the string is forced to vibrate longitudinally along its length at one of these natural frequencies, it will resonate with amplitude increasing to large values.

In the case of deuterons in the  $\delta$  phase, the fundamental frequency  $(1/2\pi) \cdot (k/m)^{1/2}$  is its thermal vibration frequency, determined from experimental measurements. Table B1 in the appendix B lists fundamental thermal vibrational frequencies  $f_0$  of isotopes of hydrogen in palladium under various conditions (phases) from the literature as well as the thermal vibration frequency of Pd. These do not account for the string nature, as in this model, but only account

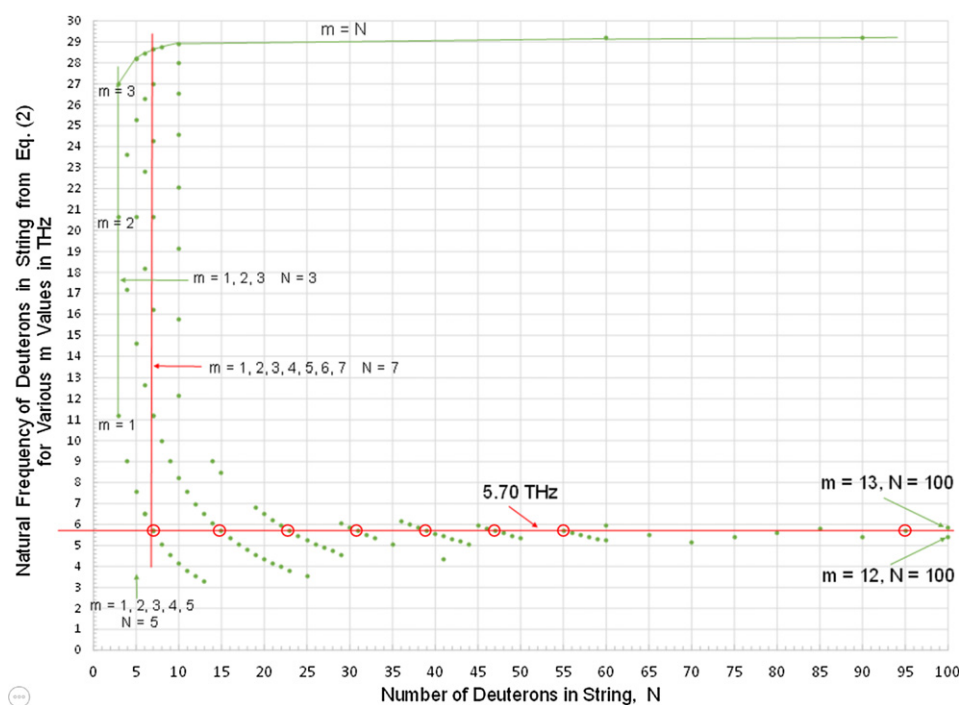


**Figure 2.** The values from the model using equation (2) of natural frequencies  $f$  (normal modes of longitudinal vibration) of any given length of a string of  $N$  ions with  $m$  modes of resonances, using  $f = (1/2\pi) \cdot \omega$  and  $f_0 = (1/2\pi) \cdot (k/m)^{1/2}$ . Each dot is a normal mode of vibration and possible natural frequency resonance if forced to vibrate at that frequency. The thermal vibration frequency of the Pd lattice is shown at 5.70 THz (see table B1 in the appendix B). The dots with circles are driven to resonance by the Pd atom at the end of the string. There are other solutions to equation (2) but only selected most relevant ones are shown near 5.70 THz. The minimum number of ions  $N$  to give a match to the frequency of the Pd vibration is  $N = 7$ , with other matches at  $N = 15, 23, 31, 39, 47, 55, 63, 71, 79, 87, 95 \dots$  etc indicted with circles.

for isolated single ions of isotopic hydrogen in their respective lattice positions. The consequences, of this model with string geometry, are extra natural frequencies, from equation (2) and figure 2 in addition to those fundamental ones in table B1.

These strings are a result of the unique lattice geometry of SAV channels in  $\delta$  phase shown in figure 3 where both lattices of beta ( $\beta$ ) deuteride of Pd–D and  $\delta$  of Pd<sub>3</sub>VacD<sub>4</sub> are compared. Here a (001) plane is shown with 6 unit cells of  $\delta$  phase in [100] direction sandwiched between  $\beta$  phase. Repeats of unit cells in [010] and [001] directions are not shown, but the model applies in all 3 orthogonal directions (orthogonal strings of deuterons intersect at corners of each unit cell). The comparison of a string of deuterons in [100] direction of  $\delta$  phase to the one dimensional Bravais lattice of ions is shown in figure 4, and suggests equation (2) of the one dimensional Bravais lattice, be used to model  $\delta$  phase.

The uniqueness of  $\delta$  phase with ordered Vac<sup>-</sup> at corners of unit cells supports this correlation to the one dimensional Bravais lattice of ions, and its description by equation (2). Density function perturbation theory (DFT) [12, 15–21] shows there is a binding energy between positively charged deuterons and Vac<sup>-</sup>, indicating negative charge associated with Vac<sup>-</sup>. Pd atoms

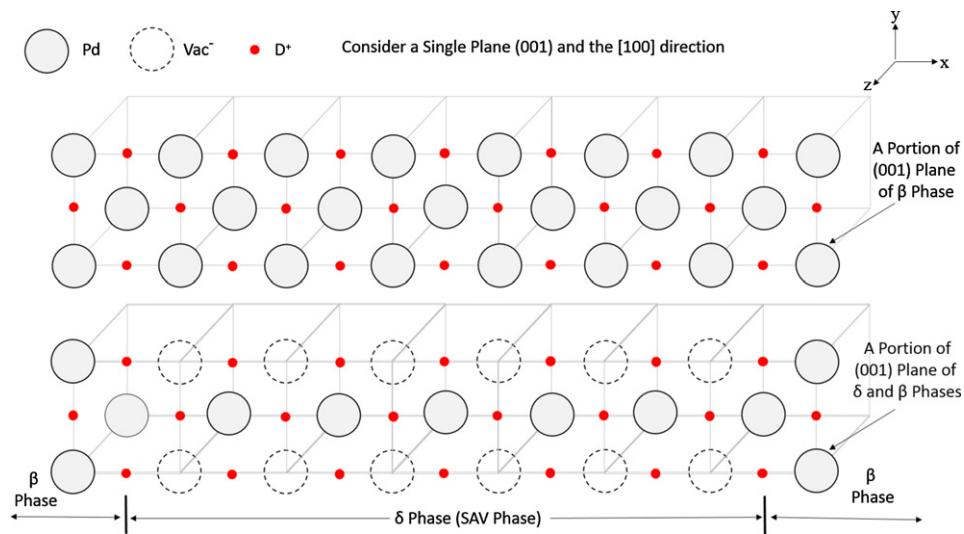


**Figure 3.** A comparison of the (001) planes of  $\beta$  phase with a D/Pd ratio of 1.0 (top) to that of a two phase microstructure of  $\delta$  phase between a matrix phase of  $\beta$  phase (bottom). The large diameter solid atoms are Pd, the vacancies (Vac) are dotted (corner positions in the fcc unit cell) and the red ions are deuterons occupying the octahedral interstitial sites.

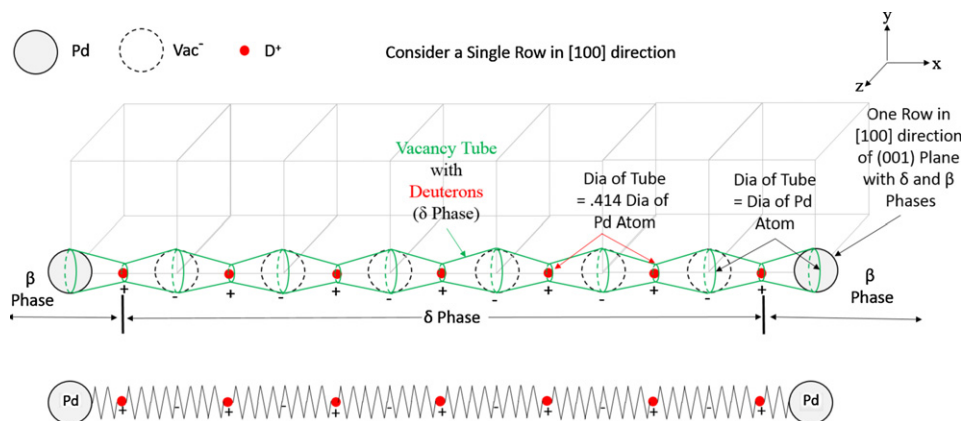


**Figure 4.** A comparison of the [100] direction of the (001) planes of  $\delta$  phase with deuterons (red) and vacancies (dotted) to that of the one-dimensional Bravais lattice of ions connected with springs and with Pd atoms on each extreme end of the string of ions to fix the ends of the extreme springs. The vacancy channel (green tube) is shown with a varying diameter of between 0.414 and 1.0 of that of the Pd atom diameter ( $2.75 \times 10^{-10}$  m). To match the solution of equation (2) one end is fixed by the Pd atom (as in figure 1(b)) and the other end is forced to vibrate by the Pd atom at that end.

from  $\beta$  phase fix the end springs because they are 52.8 times more massive and their thermal vibration frequency is lower, but can also exert longitudinal forces on the deuteron string

from thermal motion. As Pd atoms vibrate, the deuteron spring compresses and stretches producing Hookean forces on the string equal to displacement (vibration amplitude) times the spring force constant  $k$  of the deuteron's spring. In this model, the spring constant for deuteron springs is determined from  $f_o = (1/2\pi) \cdot (k/m)^{1/2}$ , so  $k = m \cdot 4 \cdot \pi^2 \cdot f_o^2$ . Since the fundamental frequency for deuterons in  $\delta$  phase is  $f_o = 14.59$  THz (table B1, Appendix B),  $k = 28.102$  N  $m^{-1}$ , using deuteron mass of  $3.344 \times 10^{-27}$  kg. From table B1, the amplitude of vibration of Pd is 0.107 Angstroms ( $\text{\AA}$ ) at room temperature. This amplitude ( $1.07 \times 10^{-11}$  m) times 28.102 N  $m^{-1}$  gives a force of  $3.01 \times 10^{-10}$  N exerted on the deuteron string in  $\langle 100 \rangle$  directions by Pd. Deuterons on perpendicular edges of the unit cell do not have an uninterrupted direct line of sight as they do in the channels and are not considered in this model to result in nearest neighbor forces since they are shielded by the Pd atoms at the center 1/2, 1/2, 0 of the fcc unit cell face. Additional vibration modes arise from the tube geometry, the  $\delta/\beta$  phase boundaries, and the negative charge of both  $Vac^-$  on each side of the positive deuteron (figures 3 and 4). The deuterons have a double attraction to each  $Vac^-$  on either side allowing the spring constant to maintain linearity and constancy to high values of deuteron displacement within channels ( $\langle 100 \rangle$  directions), a main feature of the model. Negative charge in the vicinity of each  $Vac^-$  screens positive deuterons approaching from opposite directions (optical mode), allowing closer approach than would be otherwise possible. Without this, spring constant  $k$  is variable and depends on the displacement, increasing as two deuterons approach one another near a *neutral* corner vacancy site due to their positively charged nuclei.

Of all the normal modes of vibration (natural frequencies) indicated from equation (2) and figure 2 of deuteron strings in  $\delta$  phase, many match the forcing vibration of the Pd atom at the end of the  $\delta$  phase. From table B1 this frequency for Pd vibration, when loaded with isotopic hydrogen, is 5.70 THz. It matches values in figure 2: the first is at  $N = 7, m = 1$  (exact match), second at  $N = 15, m = 2$  (exact), third exact match at  $N = 23, m = 3$  and fourth exact match at  $N = 31, m = 4$ . Other exact matches to natural frequency of Pd thermal vibration frequency occur at  $N$  and  $m$  pairs of: 39 and 5, 47 and 6, 55 and 7, 63 and 8, 71 and 9, 79 and 10, 87 and 11, 95 and 12... etc. This pattern continues to higher values of  $N$  and  $m$ , repeating every eighth  $N$  value. In addition, there are near matches at 14 and 2, 15 and 3, 16 and 2 etc, (from equation (2) solutions). As  $N$  increases the closeness of near matches improves until most of the values of  $m$  between the exact matches become near matches. It will be seen in the next section on simulation why near matches are effectively the same as exact matches: resonance peaks have widths in frequency that include near match values.

### 3. Simulation results with SolidWorks

Since figure 2 (equation (2)), shows many matches of natural frequencies to Pd at 5.70 THz, a commercial software package called SolidWorks was utilized to verify if these predictions, with large values of amplitude of vibration of deuterons (resonances), could be simulated. The geometry of a ball (mass) and spring model of figure 4 was implemented in the new feature of SolidWorks, *motion analysis simulation*. Models with 1, 3, 7, 10 deuterons, and other values of  $N$  in the string, were executed with results shown in figure 5 through 8 for 1, 3, 10 and 7 deuterons, respectively. These figures show deuteron vibration resulting from affectedly induced frequencies of vibration of the Pd atom at the end of the string. Figure 5 represents Pd vibrating at the fundamental frequency of the deuterons: it can only have a resonance if the Pd were to vibrate in the vicinity of 14.59 THz which is not the real value of vibration of Pd (5.70 THz). This simulation with one deuteron was performed as a control simulation, testing

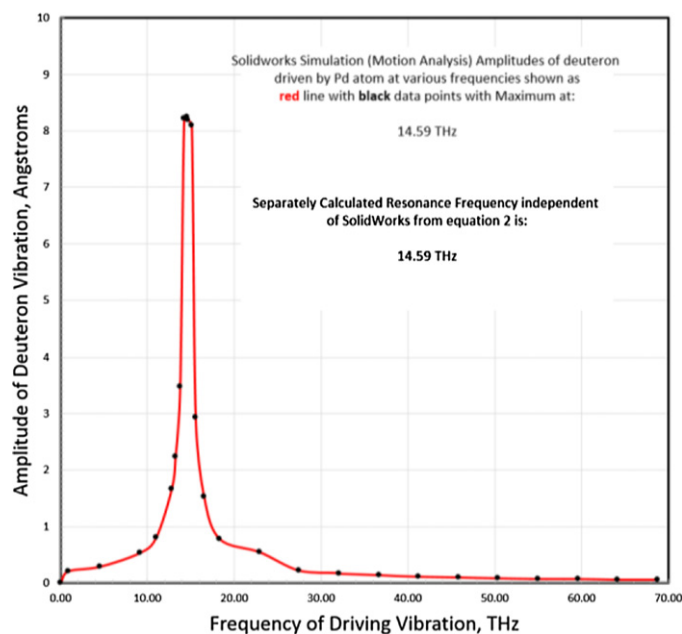


**Figure 5.** Amplitude of vibrations of a single deuteron in  $\delta$  phase driven by Pd atom vibrating at various frequencies  $f$ . The peak at 14.59 THz is the fundamental natural resonance frequency and demonstrates the effectiveness of SolidWorks to replicate this normal mode.

effectiveness of SolidWorks to replicate a known natural frequency. Figure 6 shows three resonances of deuterons at which are also not near that of Pd, but are consistent with the model (no dots in figure 2 at  $N = 3$  are close to 5.70 THz). These resonances cannot be triggered by Pd at 5.70 THz. Figure 7 for a string of 10 deuterons (1000 unit cells of  $\delta$ ) shows 10 resonances ( $1 \leq m \leq 10$ ) none of which perfectly coincide with the thermal vibration of Pd at 5.7 THz: there is an amplitude minimum between that for  $m = 1$  (at 4.153 THz) and  $m = 2$  (at 8.221 THz). However these resonance peaks, due to their widths, almost capture 5.70 THz. As  $N$  gets larger the peaks (from equation (2)) near 5.70 THz more nearly overlap the value of 5.70 THz (referred to as ‘near matches’ in the previous section). Figure 8 shows a resonance peak centered on Pd vibration frequency of 5.70 THz with half max width on both sides of this frequency. This resonance peak coincides exactly with the model prediction (figure 2 with  $N = 7$  and  $m = 1$ ), demonstrating Pd atoms do induce resonances at exact matches (and by extension of peak widths, at near matches).

In addition to amplitude of vibration, the velocity of the deuterons were measured in this study. Figure 9(a) shows the velocity of deuteron 7 with respect to deuteron 6. A similar result was obtained for deuteron 3 with respect to deuteron 2. This relative velocity shows the deuterons are effectively vibrating in an optical mode (nearly 180 degrees out of phase) when their relative velocities are near max or min in figure 9(a) (they are separating at positive values and approaching at negative values). They are in acoustical mode when their relative velocities are near zero. Over time they switch back and forth from optical to acoustical mode. From figure 9(a), it can be seen that they approach one another at a velocity of  $8.75 \times 10^5$  m s<sup>-1</sup>, however it is possible the relative velocity can be as high as twice the absolute velocity (neighboring deuterons completely out of phase), and figure 9(b) would indicate this to be as

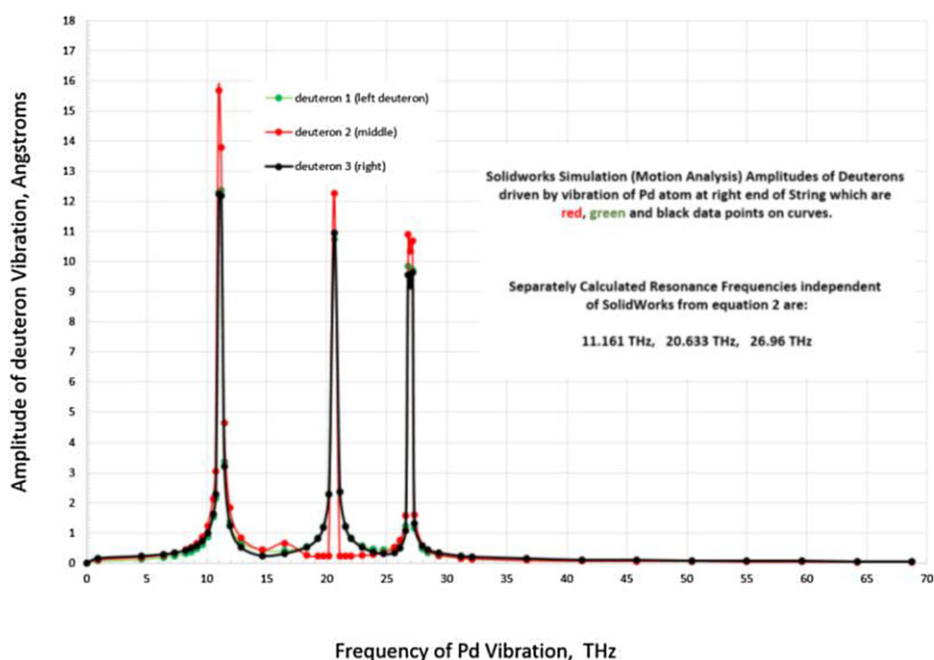


**Figure 6.** Amplitude of vibrations of three deuterons in a string on edge of SAV unit cell ( $\delta$  phase) due to Pd end atom vibration at various frequencies. None of these resonance frequencies match the thermal vibration frequency of Pd at 5.70 THz.

high as  $1.16 \times 10^6$  m s<sup>-1</sup> or slightly higher since the peak velocity appears to be still increasing at 40 picoseconds.

#### 4. Discussion

This model has several simplifying assumptions that suggest that a more sophisticated approach could reveal additional details. For example, DFT would elucidate the shielding ability of the charge of the Vac<sup>-</sup> for deuterons approaching one another on opposite sides of the Vac<sup>-</sup> and its effect on the spring constant. DFT could also examine how effective the deuterons on mutually perpendicular edges of the unit cell are shielded by both Pd atoms at the center of the face of the unit cell, 1/2, 1/2, 0, of the (001) plane and by the negative charge of the corner Vac<sup>-</sup>. Note that the deuteron at the octahedral site at the body center of the unit cell, 1/2, 1/2, 1/2, is adequately shielded from the deuterons on the octahedral sites on unit cell edges, being completely blocked by Pd atoms in nearest neighbor positions. DFT would handle the dynamics and effectiveness of the negative charge of the Vac<sup>-</sup> to shield the interaction of orthogonal strings along mutually perpendicular edges (i.e. [100] and [010], or [100] and [001] or [010] and [001] directions) of each unit cell (i.e. allowing the motion and resonance of mutually perpendicular strings to be independent of one another, or indicate specific interaction). In depth work is underway to address these, but insights gained by this model and simulation may motivate and steer future work on this phenomenon.

The possibility of buckling of the deuteron string in delta phase was compared to buckling in a model of deuterons in a crack [22, 23]. Here, delta phase geometry restrains buckling because (a) positive deuterons move inside a symmetric tube (figure 4) having an inside surface with

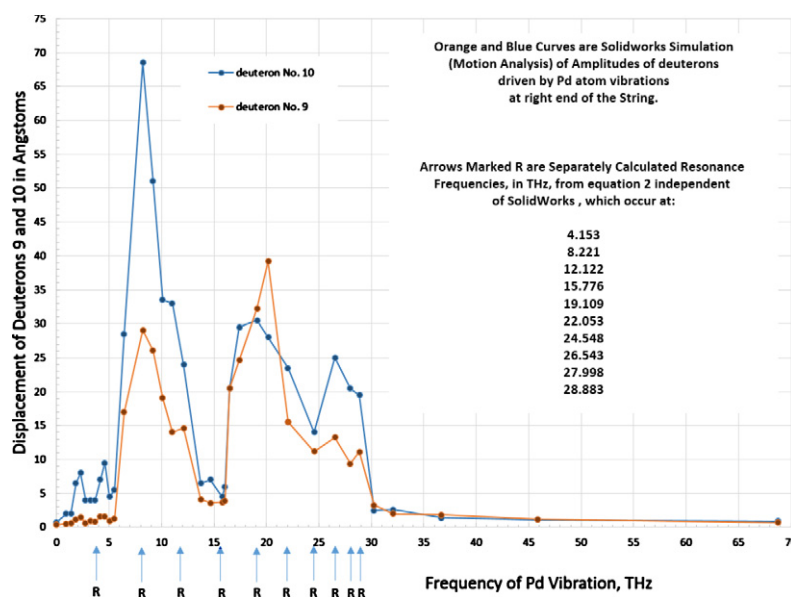


**Figure 7.** Amplitude of vibrations of ten deuterons in string on edge of SAV unit cell ( $\delta$  phase) due to Pd end atom vibration at various frequencies. None of these resonance frequencies exactly match the thermal vibration frequency of Pd at 5.70 THz.

negative charge as a result of the electrons from the surrounding Pd atoms, and this negative charge supports alignment by *pushing* them inward toward the center of the tube, (b) deuterons gain considerable velocity, as indicated in figure 9 (b) as they approach the vacancy site at the corner lattice position, and this momentum discourages transverse motion especially where most needed, near the vacancy, and (c) the deuteron's attraction to the negative vacancy site deters transverse motion by *pulling* them inward toward the center of the vacancy. Future DFT calculations may also illuminate these effects.

In this model and in the simulations one end of the string of deuterons is considered fixed while the other end undergoes vibration from the Pd atom. These conditions which fit equation (2) are preserved when both end Pd atoms vibrate if the string has double length ( $a \cdot [2 \cdot N + 1]$ ), wherein the central ion is immobile (from symmetry). Simulation runs in SolidWorks with this geometry of double length confirm the central deuteron is indeed motionless even without constraint due to symmetric stimulation (loading). Thus the double length condition for  $N = 7$  becomes two collinear and contiguous stings, each with 7 deuterons, connected by a stationary deuteron in the middle, with the right set of deuterons loaded on its right end and the left set loaded on its left end, thus each set satisfies equation (2) and the associated SolidWorks simulations reported here.

Resonance theory indicates that resonances should occur at very small amplitudes of driver vibrations when dampening is zero, as in this model. Work is underway to address effects of dampening. In this model the force exerted by thermal vibration of Pd on the ends of  $\delta$  phase (at  $\beta$  phase border) is about  $3 \times 10^{-10}$  N, determined from product of spring constant ( $28.101 \times 10^{-10}$  N m $^{-1}$ , above) times Pd vibration amplitude. Resonance, solely from thermal vibration, occurs over a range of values used in this study with specific values in figures 5–8. Values of forces in figures 5 and 6 were  $2 \times 10^{-10}$  N and figures 7 and 8 were  $18 \times 10^{-10}$  N and  $20 \times 10^{-10}$  N respectively, and in all resonances induced solely from thermal motion of Pd atoms as

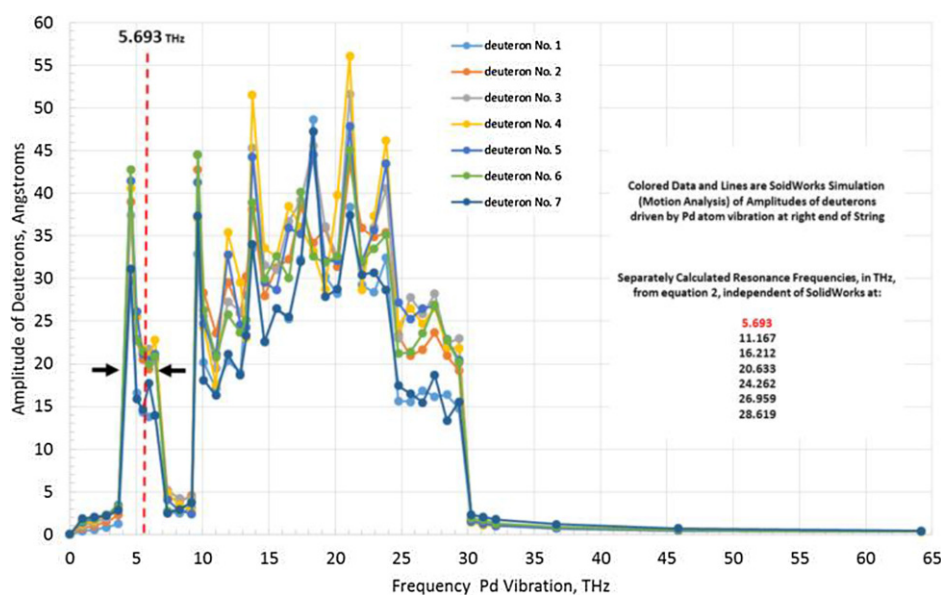


**Figure 8.** Amplitude of vibrations of seven deuterons in string on edge of SAV unit cell ( $\delta$  phase) due to Pd end atom vibration at various frequencies. The first peak ( $m = 1$ ) at 5.693 THz matches (approximate midpoint of half width) the thermal vibration frequency of Pd (5.70 THz). If peak widths are taken into account, other peaks ( $2 \leq m \leq 7$ ) also match calculated resonance frequencies; but as  $m$  increases the peak widths overlap one another.

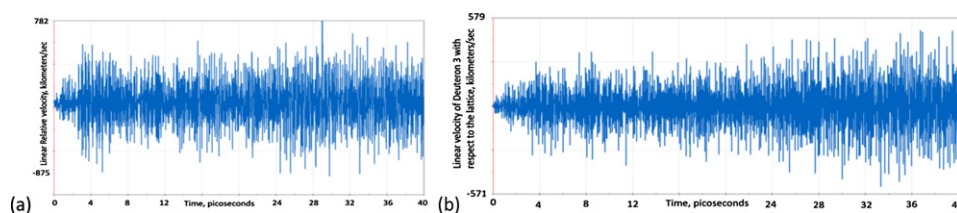


**Figure 9.** (a) Velocity of deuteron 7 with respect to deuteron 6. A similar result is observed at a frequency of 5.70 THz for deuteron 3 with respect to deuteron 2 and in general any selected set of deuterons at all the seven resonances indicated in figure 8. (b) Velocity of deuteron 3 with respect to the lattice (absolute velocity). Both (a) and (b) are for a seven deuteron string due to Pd end atom vibration at a frequency of 21.28 THz.

indicated in figure 2 at circled dots such as  $N = 7$ ,  $m = 1$  etc. Acoustic phonons from the Pd lattice feed the necessary energy for the mixed acoustic and optic modes of deuterons leading to these resonances.

## 5. Conclusions

This model and simulation suggest SAV  $\delta$  phase crystallography offers a unique geometry for vibrations of deuterons. The results suggest that as the size of  $\delta$  phase  $(N \cdot a_\delta)^3$  increases, the opportunity for high amplitude vibrations of deuterons increases because of near matches

(overlapping resonance peak widths). As the temperature of the Pd host increases, the amplitude of Pd vibration increases, making the possibility of resonance more likely due to a stronger driving force. SolidWorks simulations confirm predictions in the one dimensional Bravais lattice model, validating cases with, and cases that lack, resonance from thermal vibration of Pd atoms.

## Appendix A. SolidWorks reference information

SolidWorks version 2018 was used with scale factors of: distance =  $10^7$ , mass = 2.990430  $\times 10^{26}$ , force =  $10^{10}$ , spring constant =  $10^3$ , frequency =  $1.09084 \times 10^{-12}$ . *Motion analysis simulation* settings were: accuracy = 0.00000001, frames/s = 300, resolution = 50%, and computational times = 5 to 40 s with personal computer real run times lasting about 2 hours for each individual simulation condition.

**Table B1.** Frequency of vibration  $f_0$  of isotopic hydrogen (H or D) and palladium (Pd) under various conditions.

Element or isotope and its arrangement or state	Frequency $f_0$ (THz)	Amplitude of vibration (Angstroms)	PdA <sub>x</sub> or Pd <sub>3</sub> VacA <sub>4</sub> (A = H or D); phase = $\alpha$ , $\beta$ , $\delta$ , or $\delta'$ ; $x = A/Pd$	Temperature (K); ( $P =$ pressure, GPa)	Reference	
<b>D in <math>\delta_D</math> phase (Pd<sub>3</sub>VacD<sub>4</sub>)</b>	<b>14.59</b>		$\delta$ , $x = 1.33$	295	15 & This work	
<b>D in <math>\delta'_D</math> phase (Pd<sub>3</sub>VacD<sub>4</sub>)</b>	27.86		$\delta'$ , $x = 1.33$	295		
<b>D in Pd at octahedral sites (PdD<sub>3</sub> Phase)</b>	9.52	0.161	$\beta$ , $x = 0.63$	295	31 (Figure.3)	
	9.00		$\beta$ , $x = -0.9$	295	32	
	9.50		$\beta$ , $x = 0.63$	295	33	
	9.16		$\beta$ , $x = 0.63$	295	34	
	9.21		$\beta$ , $x = 0.75$	295	34	
	9.41		$\beta$ , $x = 0.90$	295	34	
	9.19		$\beta$ , $x = 0.63$	80	35	
	9.60		$\beta$ , $x = 0.75$	<50 and 84	36	
	9.60		$\beta$ , $x = 0.75$	20 and 78	37	
	8.95		$\beta$ , $x = -1.0$	5	38	
	Average $\beta_D = 9.30$ THz		9.15	$\beta$ , $x = 0.78$	75-85	39
			11.61	$\alpha$ , $x = 0.002$	295	40
	Average $\alpha_D = 11.43$ THz		11.24	$\alpha$ , $x = 0.014$	295	33
<b>H in <math>\delta_H</math> phase (Pd<sub>3</sub>VacH<sub>4</sub>)</b>	22.0		$\delta$ , $x = 1.33$	295	15	
<b>H in <math>\delta'_H</math> phase (Pd<sub>3</sub>VacH<sub>4</sub>)</b>	42.0		$\delta'$ , $x = 1.33$	295	15	
<b>H in Pd at octahedral sites (PdH<sub>3</sub> Phase)</b>	13.54	0.24 in [100] direction	$\beta$ , $x = 0.63$	295	41	
	13.99		$\beta$ , $x = 0.63$	295	31	
	13.78		$\beta$	295	42	
	14.24		$\beta$ , $x = 0.63$	295	33	
	13.90		$\beta$ , $x = 0.70, 0.85, 0.93$	80 and 100	43	
	14.85		low T. $\beta$ , $x = 0.0011$	5	44	
	13.36		$\beta$ , $x = 0.63$	80	45	
	14.02		$\beta$ , $x = 0.70$	70	46	
	14.15		$\beta$ , $x = 0.75$	<50 and 84	36	
	14.17		$\beta$ , $x = 0.63$	4	47	
	Average $\beta_H = 14.02$ THz		14.27	low T. $\beta$ , $x = 0.0008$	4	47
			16.44	$\alpha$ , $x = 0.03$	623	48
			15.96	$\alpha$ , $x = 0.015$	295	47
			16.26	$\alpha$ , $x = 0.0008$	295	47
			16.68	$\alpha$ , $x = 0.002$	295	40
			16.49	$\alpha$ , $0.002 \leq x \leq 0.014$	295	33
	Average $\alpha_H = 16.38$ THz		16.44	$\alpha$ , $x = 0.0011$	300	44
		$\alpha$ , $0.05 \leq x \leq 0.091$	5	38		
<b>Pd lattice atoms in PdA<sub>x</sub> (A = H or D)</b>	5.50	0.100	$\beta$ , $x = 0.63$ (A = D)	295	31	
	6.25		$\beta$ , $x = 0.63$ (A = H)	295	41	
	5.37		$\beta$ , $x = 0.63-0.90$ (A = D)	295	34	
	Average = 5.70 THz		0.113	$\alpha$ , $x = 0.007$ (A = H)	295	49
<b>Pd lattice atoms without H or D (pure Pd)</b>	6.78	0.10	$x = 0$	300	31	
	Average = 6.74 THz	0.131	$x = 0$	295	49	
	6.70		$x = 0$	296	50, 51	
For comparison, reference frequencies (THz) for solid, liquid, and gas hydrogen isotopes						
<b>D<sub>2</sub> Solid</b>	89.3			300 ( $P = 150$ GPa)	52	
	89.5			300 ( $P = 303$ GPa)	53-55	
	89.6			38	54	
	89.7			295	54, 56	
<b>H<sub>2</sub> Solid</b>	122			300 ( $P = 150$ GPa)	52	
	124			13	57	
	124			14	57	
	125			295	54, 56	

## Appendix B. Frequency of vibration of isotopic hydrogen and palladium under various conditions

Table B1 lists fundamental frequency  $f_0$  of isotopes of hydrogen (H and D) and palladium (Pd) in various phases. Both Pd–H and Pd–D exist as  $\alpha$ ,  $\beta$ ,  $\delta$ , and  $\delta'$  with a range of H/Pd or D/Pd ratios ( $x$  values). The solid, liquid and gas phases are listed for comparison and completeness. Both H and D have different values of  $f_0$  depending if the hydride PdH $_x$  or deuteride PdD $_x$  is  $\alpha$  (low  $x$ ) or  $\beta$  ( $x \geq 0.63$ ) or  $\delta$  ( $x = 1.33$ , Pd $_3$ VacA $_4$ , where A = H or D in octahedral sites) or  $\delta'$  ( $x = 1.33$ , Pd $_3$ VacA $_4$ , with A in tetrahedral sites). Since suitable amount of data is available from the literature in most cases, averages within a given data set are used in the model and simulations of this paper and listed in table B1. For example using average values, the ratio of the  $f_0$  of  $\beta_H/\beta_D = 1.51$  and  $f_0$  of  $\alpha_H/\alpha_D = 1.43$  compared to the inverse mass ratio 1.41. The ratio for  $f_0$  of  $\delta_H/\delta_D$  is 1.51 (because of reason give below). The  $f_0$  of H in  $\delta$  and  $\delta'$  are reported in reference 15 giving  $f_0$  of  $\delta_H/\beta_H = 1.57$ , however  $f_0$  of D in  $\delta$  and  $\delta'$  are not reported in reference [15]. This same ratio (1.57) was used to set  $\delta_D/\beta_D$  at 1.57, since the  $f_0$  of  $\delta_H/\delta_D$  is assumed to be better represented by  $f_0$  of  $\beta_H/\beta_D$  than by  $f_0$  of  $\alpha_H/\alpha_D$ , because both  $\beta$  and  $\delta$  have high  $x$  values). Thus the first two entries in table B1 are from values from reference [15] and the use of this ratio (1.57) from the observations of the present work (including all the data from table B1 taken as a whole).

### ORCID iDs

M R Staker  <https://orcid.org/0000-0002-5003-8459>

### References

- [1] Fukai Y and Okuma N 1993 Evidence of copious vacancy formation in Ni and Pd under a high hydrogen pressure *Japan. J. Appl. Phys.* **32** 1256
- [2] Oates W A and Wenzl H 1994 On the copious formation of vacancies in metals *Scr. Metall. Mater.* **30** 851–4
- [3] Oates W A and Wenzl H 1995 On the formation and ordering of superabundant vacancies in palladium due to hydrogen absorption *Scr. Metall. Mater.* **33** 185–93
- [4] Fukai Y 2005 *The Metal–Hydrogen System: Basic Bulk Properties* 2nd edn (Berlin: Springer)
- [5] Fukai Y 2003 Superabundant vacancies formed in metal–hydrogen alloys *Phys. Scr.* **T 103** 11
- [6] Degtyareva V F 2009 Electronic origin of superabundant vacancies in Pd hydride under high hydrogen pressures *Presented on the Conf. on Hydrogen Materials Science (ICHMS) (Yalta, Ukraine)* pp 25–31
- [7] Tanguy D and Mareschal M 2005 Superabundant vacancies in a metal–hydrogen system: Monte Carlo simulations *Phys. Rev. B* **72** 174116
- [8] Fukai Y 2011 Hydrogen-induced superabundant vacancies in metals: implication for electrodeposition *Defect Diffus. Forum* **312–315** 1106–15
- [9] dos Santos D S, Miraglia S and Fruchart D 1999 A high pressure investigation of Pd and the Pd–H system *J. Alloys Compd.* **291** L1–5
- [10] Fukai Y and Okuma N 1994 Formation of superabundant vacancies in Pd hydride under high hydrogen pressures *Phys. Rev. Lett.* **73** 1640–3
- [11] Fukada Y, Hioki T and Motohiro T 2016 Multiple phase separation of super-abundant-vacancies in Pd hydrides by all solid-state electrolysis in moderate temperatures around 300 C *J. Alloys Compd.* **688** 404–12
- [12] Zhang C and Alavi A 2005 First-principles study of superabundant vacancy formation in metal hydrides *J. Am. Chem. Soc.* **127** 9808–17
- [13] Fukai Y, Mizutani M, Yokota S, Kanazawa M, Miura Y and Watanabe T 2003 Superabundant vacancy–hydrogen clusters in electrodeposited Ni and Cu *J. Alloys Compd.* **356–357** 270

- [14] Fukai Y 2003 Formation of superabundant vacancies in M–H alloys and some of its consequences: a review *J. Alloys Compd.* **356–357** 263–9
- [15] Isaeva L E, Bazhanov D I, Isaev E, Ereemeev S V, Kulkova S E and Abrikosov I 2011 Dynamic stability of palladium hydride: an *ab initio* study *Int. J. Hydrogen Energy* **36** 1254–8
- [16] Fukai Y and Sugimoto H 2007 Formation mechanism of defect metal hydrides containing superabundant vacancies *J. Phys.: Condens. Matter* **19** 436201
- [17] Sugimoto H and Fukai Y 2009 Migration mechanism in defect metal hydrides containing superabundant vacancies *Diffusionfundamentals.org* **11** 1–2
- [18] Bukonte L, Ahlgren T and Heinola K 2017 Thermodynamics of impurity-enhanced vacancy formation in metals *J. Appl. Phys.* **121** 045102
- [19] Fukai Y and Sugimoto H 2007 The defect structure with superabundant vacancies to be formed from fcc binary metal hydrides: experiments and simulations *J. Alloys Compd.* **446–447** 474–8
- [20] Nazarov R, Hickel T and Neugebauer J 2014 *Ab Initio* study of H-vacancy interactions in fcc metals: implications for the formation of superabundant vacancies *Phys. Rev. B* **89** 144108
- [21] Fukai Y, Kurokawa Y and Hiraoka H 1997 Superabundant vacancy formation and its consequences in metal hydrogen alloys *J. Japan Inst. Met.* **61** 663–70 (in Japanese)
- [22] Staker M R 2019 Coupled calorimetry and resistivity measurements, in conjunction with an emended and more complete phase diagram of the palladium - isotopic hydrogen system *J. Cond. Matter Nucl. Sci.* **29** 129–68
- [23] Staker M R 2020 Estimating volume fractions of superabundant vacancy phases and their potential roles in low energy nuclear reactions and high conductivity in the palladium–isotopic hydrogen system *Mat. Sci. Eng. B* (accepted)
- [24] Pitt M P and MacA Gray E 2003 Tetrahedral occupancy in the Pd–D system observed by *in situ* neutron powder diffraction *Europhys. Lett.* **64** 344–50
- [25] Ferguson G A Jr, Schindler A I, Tanaka T and Morita T 1965 Neutron diffraction study of temperature-dependent properties of palladium containing absorbed hydrogen *Phys. Rev.* **137** 483
- [26] McLennan K G, Gray E MacA and Dobson J F 2008 Deuterium occupation of tetrahedral sites in palladium *Phys. Rev. B* **78** 014104
- [27] Ashcraft N W and Mermin N D 1976 *Solid State Physics* (Orlando, FL: Harcourt College Publishers) p 432
- [28] Kittel C 2005 *Introduction to Solid State Physics* 8th edn (New York: Wiley) pp 108–10
- [29] Torre C G 2016 *Foundations of Wave Phenomena: Complete Version (8.3)* (Department of Physics, Utah State University) pp 29–31 ([https://digitalcommons.usu.edu/foundation\\_wave/](https://digitalcommons.usu.edu/foundation_wave/) accessed 17 Jan 2020)
- [30] Dean P 1967 Atomic vibrations in solids *IMA J. Appl. Math.* **3** 98–165
- [31] Rowe J M, Rush J J, Smith H G, Mostoller M and Flotow H E 1974 Lattice dynamics of a single crystal of PdD<sub>63</sub> *Phys. Rev. Lett.* **33** 1297–300
- [32] Kuzovnikov M A 2020 Vibrational properties of H impurity in high-pressure palladium deuteride *Institute Solid State Phys. Russian Acad. Sci., Chernogolovka* (<https://kuz@issp.ac.ruhttps://issp.ac.ru/lhpp/PapersKuzovnikov/Kuz4.pdf>)
- [33] Rush J J, Rowe J M and Richter D 1984 Direct determination of the anharmonic vibrational potential for H in Pd *Z. Phys. B* **55** 283–6
- [34] Sansores L E, Tagueiia-Martinez J and Tahir-Kheli R A 1982 Lattice dynamics of PdD, and PdH *J. Phys. C: Solid State Phys.* **15** 6907–17
- [35] Glinka C J, Rowe J M, Rush J J, Rahman A, Sinha S K and Flotow H E 1978 Inelastic-neutron-scattering line shapes in PdD<sub>63</sub> *Phys. Rev. B* **17** 488–93
- [36] Sherman R, Birnbaum H K, Holy J A and Klein M V 1977 Raman studies of hydrogen vibrational modes in palladium *Phys. Lett. A.* **62** 353–5
- [37] Sherman R 1978 Raman studies of hydrogen vibrational modes in palladium *Master of Science Thesis in Metallurgical Engineering* University of Illinois at Urbana-Champaign
- [38] Antonov V E, Davydov A I, Fedotov V K, Ivanov A S, Kolesnikov A I and Kuzovnikov M A 2009 Neutron spectr. of H Impurities in PdD Covibratins of the H and D Atoms *Phys. Rev. B* **80** 134302
- [39] Blaschko Q, Klemencic R, Weinzier P and Pintschovius L 1981 Lattice dynamics of  $\beta$ -PdD<sub>78</sub> at 85 K and ordering effects at 75 K *Phys. Rev. B* **24** 1552–5
- [40] Drexel W, Murani A, Tocchetti D, Kley W, Sosnowska I and Ross D K 1976 The motions of hydrogen impurities in alpha-palladium-hydride *J. Phys. Chem. Solids* **37** 1135–9

- [41] Bergsma J and Goedkoop J A 1960 Thermal motion in palladium hydride studied by means of elastic and inelastic scattering of neutrons *Physica* **26** 744–50
- [42] Chowdhury M R and Ross D K 1973 A neutron scattering study of the vibrational modes of hydrogen in the  $\beta$ -phases of Pd–H, Pd-10Ag–H and Pd-20Ag–H *Solid State Commun.* **13** 229–34
- [43] Ross D K, Martin P F, Oates N A and Khoda Bakhsh R 1979 Inelastic neutron scattering measurements of optical vibration frequency distributions in hydrogen-metal systems *Z. Phys. Chem., Neue Folge* **114** 221–30
- [44] Yang T-N 2013 Trapped hydrogen vibrational density of states measurement using IINS PdH<sub>0.0011</sub> at 5 K and 300 K with incident neutron energy of 250 Mev *Master of Science Thesis* University of Illinois at Urbana-Champaign
- [45] Rahman A, Skold K, Pelizari C, Sinha S K and Flotow H E 1976 Photon spectra of non-stoichiometric Pd hydrides *Phys. Rev. B* **14** 3630–4
- [46] Hunt D G and Ross D K 1976 Optical vibrations of H in metals *J. Less Common Met.* **49** 169–91
- [47] Heuser B J, Udovic T J and Ju H 2008 Vibrational density of states measurement of hydrogen trapped at dislocations in deformed PdH<sub>0.0008</sub> *Phys. Rev. B* **78** 214101
- [48] Rowe J M, Rush J J, de Graaf L A and Ferguson G A 1972 Neutron quasielastic scattering study of hydrogen diffusion in a single crystal of palladium *Phys. Rev. Lett.* **29** 1250–3
- [49] Owen E A and Evans E W 1967 The effect of the occlusion of hydrogen on the characteristic temperature of palladium and the vibration amplitudes of its atoms *Br. J. Appl. Phys.* **18** 605–10
- [50] Miiller A P and Brockhouse B N 1968 Anomalous behavior of the lattice vibrations and the electronic specific heat of palladium *Phys. Rev. Lett.* **20** 798–801
- [51] Miiller A P and Brockhouse B N 1971 Crystal dynamics and electronic specific heats of palladium and copper *Can. J. Phys.* **49** 704–23
- [52] Dalladay-Simpson P, Howie R T and Gregoryanz E 2016 Evidence for a new phase of dense hydrogen above 325 gigapascals *Nature* **529** 63–7
- [53] Zha C-s, Cohena R E, Maoa H-k and Hemley R J 2014 Raman measurements of phase transitions in dense solid hydrogen and deuterium to 325 Gpa *Proc. Natl Acad. Sci. USA* **111** 4792–7
- [54] Centrone A, Siberio-Perez D Y, Millward A R, Yaghi O M, Matzger A J and Zerbi G 2005 Raman spectra of H and D adsorbed on a meta-organic framework *Chem. Phys. Lett.* **411** 516–9
- [55] Stoicheff B P 1957 High res. Raman spectroscopy gases: IX. Spectra H<sub>2</sub>, HD, and D<sub>2</sub> *Can J. Phys.* **35** 730–41
- [56] Dickenson G D, Niu M L, Salumbides E J, Komasa J, Eikema K S E, Pachucki K and Ubachs W 2013 Fundamental vibration of molecular hydrogen *Phys. Rev. Lett.* **110** 193601
- [57] Allin E J, Feldman T and Welsh H L 1956 Raman spectra of liquid and solid hydrogen *J. Chem. Phys.* **24** 1116–7